RAPID COMMUNICATIONS

PHYSICAL REVIEW A VOLUME 41, NUMBER 7 1 APRIL 1990

# Recombination reactions of 5-eV $O(^3P)$ atoms on a $MgF_2$ surface

O. J. Orient and A. Chutjian
*Jet Propulsion Laboratory, California Institute of Technology, Pasadena, California 91109*

E. Murad
*Space Physics Division, Geophysics Laboratory, Hanscom Air Force Base, Massachusetts 01731*

(Received 17 January 1990)

A source of hyperthermal, ground-state, impurity-free, atomic oxygen of an energy variable in the range 2–100 eV has been developed. Experimental results are presented of emission spectra in the wavelength range 250–850 nm produced by collisions of 5-eV $O(^3P)$ atoms with adsorbed NO and CO molecules on a $MgF_2$ surface. The emission with adsorbed CO is due to the $\tilde{B} \rightarrow \tilde{X}$ transition in $CO_2$, while that with NO is consistent with the continuum $\tilde{B} \rightarrow \tilde{X}$ and $\tilde{A} \rightarrow \tilde{X}$ emissions in $NO_2$.

There is currently great interest in studying collisions of fast, ground-state atomic oxygen with surfaces to access phenomena such as surface oxidation, erosion, and chemiluminescence. Hyperthermal (atom energy $E \sim 5$ eV), ground-state O atoms are thought to give rise to the so-called "Shuttle glow" phenomenon by recombination, in low-Earth orbit, with surface-adsorbed NO to form excited nitrogen dioxide ($NO_2$).[1] Measurements show a definite correlation of glow intensity with O-atom density,[2–4] while mass-spectrometric data have provided indirect evidence for the role of $NO_2$.[5] These problems led us to develop a source of fast, ground-state atomic oxygen in order to test, as part of a larger laboratory effort in atom-surface collisions, many aspects of the interaction of spacecraft with fast atomic oxygen.

We briefly describe herein a source of variable-energy, ground-state atomic oxygen based on techniques of magnetic confinement and photodetachment of $O^-(^2P)$ ions.[6] Using this atomic-oxygen beam, we have observed emission spectra produced in collisions of 5-eV atoms with a magnesium fluoride ($MgF_2$) surface having adsorbed CO and NO molecules. These are first surface-collision emission measurements of any type using a hyperthermal beam of atoms of known energy, energy width, quantum state, and purity.

A schematic diagram of the present O-atom source is given in Fig. 1. Techniques used in the source involve the following steps carried out in a uniform, high-intensity (6 T) solenoidal magnetic field: (a) generate electrons from a tungsten filament ($F$), and $O^-(^2P)$ ions via dissociative attachment to NO at 8-eV electron energy (at $G$); (b) accelerate the magnetically confined $O^-$ ions and electrons

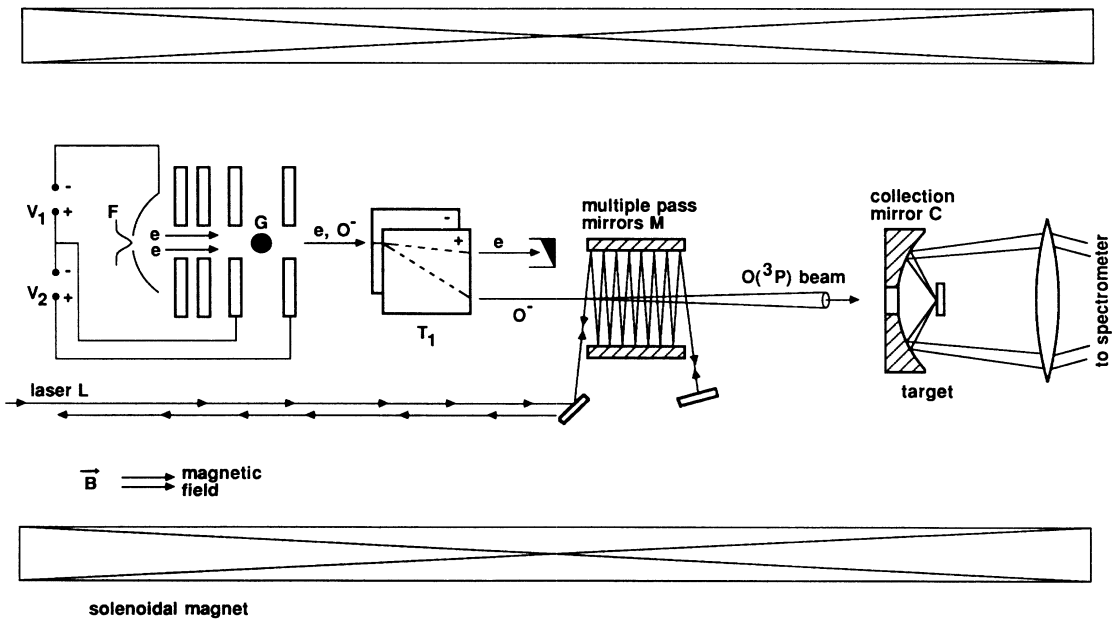


FIG. 1. Schematic diagram of the magnetically confined source used to produce ground-state atomic-oxygen atoms. See text for details.

 

to the desired final energy (5 eV, say); (c) by trochoidal deflection (at $T_1$) separate the higher-velocity electrons from the slower $O^-$ ions, and trap the electrons in their Faraday cup; (d) detach the electron from $O^-$ by a 20-W, cw argon-ion laser ($L$) and a multiple-pass mirror assembly ($M$); and (e) direct the $O^-$ and O beams toward the target (here, $MgF_2$), and reflect the undetached $O^-$ beam by biasing the target negative with respect to the $O^-$ kinetic energy. Alternatively, a second trochoidal deflector, located immediately after the mirrors $M$, was sometimes used to separate the ground-state $O(^3P)$ atoms from undetached $O^-$ ions, with the latter trapped in a separate Faraday cup for analysis of the $O^-$ beam.

The laser wavelengths are restricted to visible lines of the argon-ion laser so that detachment results in exclusively ground-state atoms.[7] For a 20-W laser, 5-eV ions, and 100 passes of the laser across the $O^-$ beam, one obtains about a 15% detachment efficiency into $O(^3P)$. The variation of detachment efficiency with $O^-$ energy was confirmed experimentally, by noting the decrease in $O^-$ current in a Faraday cup after the second trochoidal deflector. This efficiency $g$ was also calculated in terms of known experimental parameters through the expression

$$g = 1 - \exp(-f\sigma L/v) , \quad (1)$$

where $f$ is the laser flux (photons/cm$^2$s), $\sigma$ the detachment cross section (cm$^2$), $L$ the total path length in $M$ for the detachment (cm), and $v$ the $O^-$ velocity (cm/s).

The 5-eV $O^-$ ions, at sufficiently high ion currents, experience space-charge repulsion while confined by the 6-T magnetic field. In order to minimize rapid divergence of the O-atom beam after detachment, care was taken in the source to restrict the energy of the $O^-$ ions perpendicular to the $B$ field. This involved choosing the target gas at $G$ (here, nitric oxide) to provide small $O^-$ kinetic energy at the onset;[8] and by limiting $O^-$ currents to 5 $\mu$A or less at 5 eV. Simple calculation involving the balance between the repulsive force $\mathbf{F}_r = e\mathbf{E}_r$ of the radial electric field $\mathbf{E}_r$, and the centripetal force $\mathbf{F}_c = e\mathbf{v}_\theta \times \mathbf{B}$ of the confined, spiraling ions (here, $\mathbf{v}_\theta$ is their tangential velocity) provides a measure of $\mathbf{v}_\theta$ by the relation $mv_\theta^2/r = F_c - F_r$, where $r$ is the radial distance of the ion. This in turn gives an estimate of the divergence angle in the final O beam to be about 20°. The diameter of a visible, eroded area of the $MgF_2$ sample corresponded to an actual divergence angle of slightly less than this. Further details on the source will be given in a subsequent publication.

$MgF_2$ was chosen as the target because of its tendency to radiate during O-atom collisions in the low-earth orbit environment (see Ref. 4 for a summary). A 95% transmitting tungsten mesh covered its surface to allow repulsion of the $O^-$ beam during O-atom emission measurements. This mesh itself was shown not to contribute to the emission. The target was differentially pumped relative to the source region, and a pressure differential of $7\times10^{-4}$ Pa (source) and $1\times10^{-6}$ Pa (target) maintained during operation. This pumping ensured that no impurities, such as the nitric-oxide feed gas (at $G$), could reach the target.

A small gas jet (not shown in Fig. 1) was used to direct a beam of either CO or NO onto the $MgF_2$ surface in order to enhance surface-adsorbed emissions. A high-reflectivity focusing mirror at $C$ collected a broad spatial extent of the optical emissions from the target. These emissions were focused onto the entrance plane of a fast $f/3.5$ double-grating monochromator capable of attenuating by a factor $> 10^9$ laser lines at 500 nm from spectral emissions at wavelengths below 400 and above 600 nm. The photon-detection system was an RCA GaAs:CsO phototube with a manufacturer's stated long-wavelength cutoff of 900 nm. Fast, pulse-counting electronics were used, and spectra were recorded by multichannel scaling.

Optical emissions are observed when 5-eV O atoms strike the $MgF_2$ surface with the gas jet turned off. When the gas jet of either CO or NO is turned on, both the intensity and spectral distribution of the emissions change. All emissions were found to be linear in O-atom flux. That the source of the extra emissions is the target surface itself, rather than purely gas-phase collisions in front of the target is seen from two arguments. First, upon turning off the gas jet, the optical emission decays slowly relative to decay of background pressure in the target chamber. The time constant for decay of the emission is more than 1 order of magnitude greater than that of the background pressure. Second, assuming a rather large atom-gas collision cross section of $10^{-15}$ cm$^2$, using known values for the collection-solid angle of the mirror $C$, the O-atom flux, and an estimate of the detection efficiency of the monochromator and phototube, one may calculate an emission rate for the atom-gas process. This was again more than 1 order of magnitude less than the observed rates, implying that a larger gas-surface collision cross section of value greater than $10^{-14}$ cm$^2$ was involved.

Experimental results of the surface emissions when CO and NO are adsorbed onto the target are given in Fig. 2. The resolution in these measurements was 10 nm. All data were corrected for the spectral response of the photo-

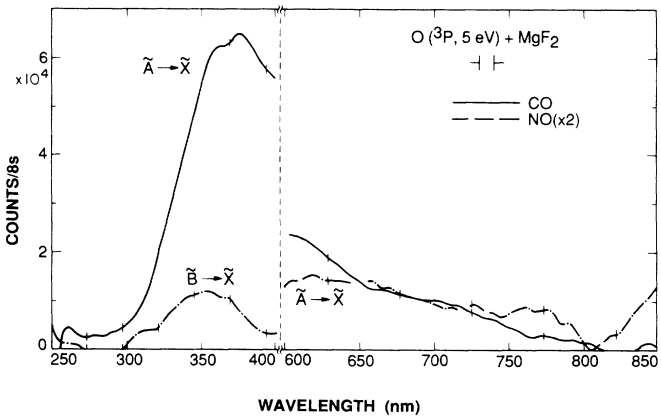


FIG. 2. Emission spectra arising from $CO_2$ (solid line) and $NO_2$ (dash-dotted line) in the wavelength range 250–850 nm produced by surface-adsorbed CO and NO on $MgF_2$. Incident particles are 5-eV $O(^3P)$ atoms striking the differentially pumped $MgF_2$ target. The NO spectral intensity has been multiplied by a factor of 2. The break in wavelength scale between 400 and 600 nm is the region of interference by scattered light from the photodetaching argon-ion laser.

tube as given by the manufacturer. One clearly sees for CO an intense emission in the wavelength range extending from 300 to > 800 nm. This range agrees qualitatively with that observed in a gas-phase, three-body recombination of O+CO.[9] The emissions in NO are weaker than for CO, and extend over the range 300 to > 850 nm, with a minimum at about 825 nm. In neither case do the emission wavelengths correspond to transitions in diatomic CO or NO.[10]

The source of the emissions in the CO case is almost certainly excited $CO_2$ molecules formed at the surface. To see this, we refer to recent, *ab initio* configuration-interaction calculations of sections of the excited potential-energy surfaces.[11] In Fig. 3 bending curves are shown for the excited and ground states calculated at the equilibrium bond angle (120°) and O-C-O internuclear separation (1.246 Å) for the $^1B_2$ state. The scenario is that O and CO recombine on the $MgF_2$ surface to form excited $CO_2$ in the $^1B_2$ state. The observed emissions then proceed through the optically allowed $\tilde{A}\,^1B_2 \rightarrow \tilde{X}\,^1A_1$ transition.[12] The Franck-Condon region is shown in Fig. 3 (shading), centered at the minimum energy of the $^1B_2$ state, consistent with the observed-emission wavelength range in Fig. 2. The potential-energy curves would also imply that the excited $CO_2$ is formed with about 0.2–0.3-eV vibrational energy.

The emissions in the case of NO show two broad maxima centered near 350 and 625 nm. There would also appear to be a third region of increased emission at wavelengths greater than 850 nm, approaching the phototube cutoff. The emission maximum near 625 nm is almost certainly due to the $\tilde{A}\,^2B_2 \rightarrow \tilde{X}\,^2A_1$ transition.[12,13] Its peak location is in qualitative agreement with observations on the Shuttle[4] showing a maximum at 680 nm, as viewed over several different Shuttle materials at different surface temperatures. Assignment of the peak at 350 nm is consistent with recombination into the $\tilde{B}\,^2B_1$ state, followed by the $\tilde{B}\,^2B_1 \rightarrow \tilde{X}\,^2A_1$ emission. Assignment of this peak follows from rotational analysis studies on the $\tilde{B} \rightarrow \tilde{X}$ transition,[13] and from extensive *ab initio* calculations of Gillespie and co-workers.[14,15]

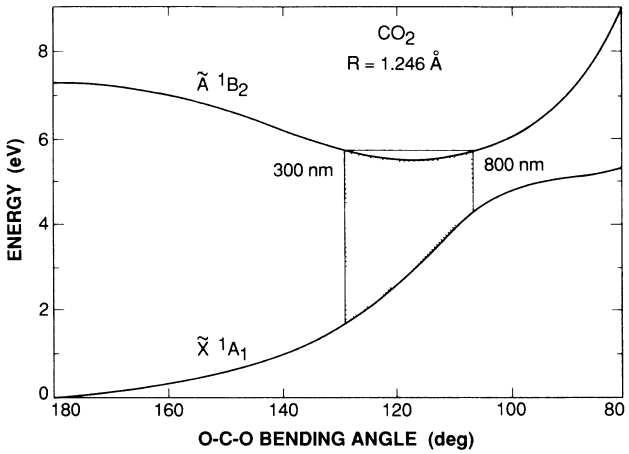


FIG. 3. Bending curves for the $\tilde{A}\,^1B_2$ and $\tilde{X}\,^1A_1$ states of $CO_2$ calculated at the equilibrium bond angle and equilibrium O-C-O distance of the $^1B_2$ state (from Ref. 11). The Franck-Condon region corresponding to the range of observed emissions in Fig. 2 is indicated by shading.

Work is continuing in this laboratory on measurement of, at higher-resolution, recombination transitions in the infrared region ($\lambda > 850$ nm), recombination on other metallic and insulator surfaces, and in measurement of surface-temperature dependencies of the emissions.

We are grateful to Dr. N. W. Winter for results of his calculations of the potential-energy surfaces of $CO_2$, and to Dr. I. L. Kofsky for several helpful discussions. This work was carried out at the Jet Propulsion Laboratory, California Institute of Technology, and was supported by Air Force Geophysics Laboratory and U.S. Defense Advanced Research Projects Agency through agreement with NASA.

[1]G. R. Swenson, S. B. Mende, and K. S. Clifton, Geophys. Res. Lett. **12**, 97 (1985).

[2]I. L. Kofsky and J. L. Barrett, Nucl. Instrum. Methods Phys. Res. Sect. B **14**, 480 (1986).

[3]E. Murad, in *Physics of Space Plasmas (1985–1987)*, edited by T. Chang, J. Belcher, J. R. Jasperse, and G. B. Crew (Scientific, Cambridge, MA, 1987), p. 147.

[4]H. B. Garrett, A. Chutjian, and S. Gabriel, J. Spacecr. Rockets **25**, 321 (1988).

[5]U. von Zahn and E. Murad, Nature (London) **321**, 147 (1986).

[6]Preliminary results of this work were presented by O. J. Orient, A. Chutjian, and E. Murad, in *Proceedings of the Fifteenth International Conference on the Physics of Electronic and Atomic Collisions, Brighton, United Kingdom, 1987*, Abstracts of Contributed papers, edited by J. Geddes *et al.* (ICPEAC, Brighton, United Kingdom, 1987), p. 813; Forty First Annual Gaseous Electronics Conference (University of Minnesota, Minneapolis, MN, 1988).

[7]L. M. Branscomb, S. J. Smith, and G. Tisone, J. Chem. Phys. **43**, 2906 (1965).

[8]P. J. Chantry, Phys. Rev. **172**, 125 (1968).

[9]A. M. Pravilov and L. G. Smirnova, Kinet. Catal. **22**, 416 (1981) (English translation).

[10]G. Herzberg, *Molecular Spectra and Molecular Structure-I. Spectra of Diatomic Molecules* (Van Nostrand, New York, 1950), pp. 452–453.

[11]N. W. Winter (private communication); N. W. Winter, C. F. Bender, and W. A. Goddard III, Chem. Phys. Lett. **20**, 489 (1973).

[12]G. Herzberg, *Molecular Spectra and Molecular Structure-III. Electronic Spectra of Polyatomic Molecules* (Van Nostrand, New York, 1966), pp. 598, 602.

[13]A. E. Douglas and K. P. Huber, Can. J. Phys. **43**, 72 (1965).

[14]G. D. Gillespie and A. U. Khan, J. Chem. Phys. **65**, 1624 (1976).

[15]G. D. Gillespie, A. U. Khan, A. C. Wahl, R. P. Hosteny, and M. Krauss, J. Chem. Phys. **63**, 3425 (1975).

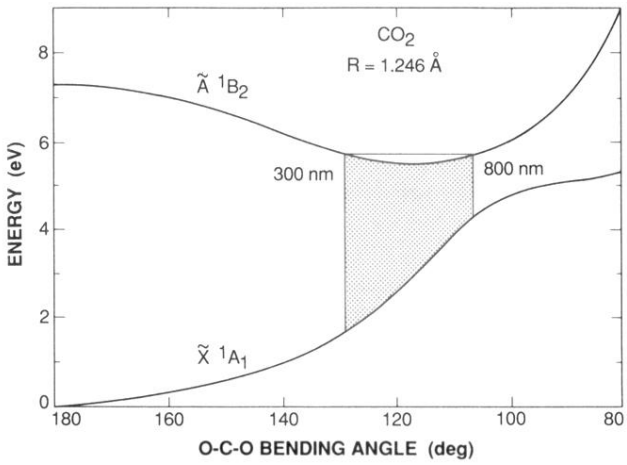


FIG. 3. Bending curves for the $\tilde{A}\,^1B_2$ and $\tilde{X}\,^1A_1$ states of $CO_2$ calculated at the equilibrium bond angle and equilibrium O-C-O distance of the $^1B_2$ state (from Ref. 11). The Franck-Condon region corresponding to the range of observed emissions in Fig. 2 is indicated by shading.